Auger recombination in low-band-gap *n*-type InGaAs

W. K. Metzger,[a] M. W. Wanlass, R. J. Ellingson, R. K. Ahrenkiel, and J. J. Carapella
National Renewable Energy Laboratory, Golden, Colorado 80401

(Received 24 January 2001; accepted for publication 20 September 2001)

We measured the recombination lifetime of degenerate n-$In_xGa_{1-x}As$ for three different compositions that correspond to $x=0.53$, 0.66, and 0.78 (band gaps of 0.74, 0.60, and 0.50 eV, respectively) over the doping range of $3\times10^{18}-5\times10^{19}$ carriers/cm^3. The Auger recombination rate increases slowly with decreasing band gap, and it matches the behavior predicted for phonon-assisted recombination. © *2001 American Institute of Physics.*
[DOI: 10.1063/1.1418032]

Low-band-gap $In_xGa_{1-x}As\,(0.53>x>1)$ can be used to make long-wavelength lasers, photodetectors, infrared photovoltaic junctions, thermophotovoltaic (TPV) energy converters, and other semiconductor devices. It is particularly attractive because it covers a band-gap region that is under development by the semiconductor laser industry and considered optimal for many TPV applications.[1]

The performance of all of the devices mentioned above is critically dependent on the recombination lifetime τ. For low-injection conditions and nondegenerate n-type material, the complex theory of electron–hole recombination in semiconductors can be represented by the parametric equation

$$\tau=[\tau_{SRH}^{-1}+Bn+Cn^2]^{-1}. \quad (1)$$

The three terms on the right-hand side of Eq. (1) represent the Shockley–Read–Hall (SRH), radiative, and Auger recombination contributions, respectively, to the total lifetime. Here, τ_{SRH} is the Shockley–Read–Hall lifetime, n is the free-electron concentration, and B and C are the radiative and Auger recombination coefficients, respectively.

The experimental values of the Auger coefficient reported by Henry *et al.* and Ahrenkiel *et al.* for 0.74 eV n-InGaAs are 5×10^{-30} and 7×10^{-29} cm^6/s, respectively.[2,3] Experimental values of the Auger coefficient reported in the literature for InAs are 1.1×10^{-26}, 1.6×10^{-27}, and 7.8×10^{-27} cm^6/s (Refs. 4–6). (The first two values were measured under high-injection conditions.)

By interpolation, one would expect that the Auger rate of recombination increases dramatically as the band gap is decreased in low-band-gap InGaAs. Such an increase would have severe effects on device performance. In semiconductor lasers, Auger recombination is one of the primary factors that determines the viability, threshold current, and maximum operating temperature.[7,8] To reduce the deleterious effects of Auger recombination on laser applications, an enormous amount of recent research has focused on quantum-cascade lasers and quantum-well structures. In infrared-detector applications, Auger recombination contributes significantly to the dark current, which limits the signal-to-noise ratio. In thermophotovoltaics, the band-gap range from 0.5 to 0.6 eV is considered optimal for thermophotovoltaic conversion. However, if the Auger coefficient is increased from the value given by Henry *et al.* for 0.74 eV InGaAs to the value given by Vodopyanov *et al.* for InAs, the theoretical efficiency of a TPV converter is estimated to decrease by a factor of 2. Because there are very few materials (InGaAs and InGaAsSb are the focus of most TPV research) that are suitable for TPV conversion, the behavior of Auger recombination for InGaAs between 0.74 and 0.50 eV is critical. Despite these implications, there have been no prior experimental studies of Auger recombination in low-band-gap InGaAs.

Epitaxial thin-film InAsP/InGaAs/InAsP double heterostructures were fabricated using atmospheric-pressure metallorganic vapor–phase epitaxy.[1] If the desired composition of InGaAs could not be grown lattice matched to the InP substrate, compositionally step-graded layers of InAsP were deposited until the desired composition of InGaAs could be grown lattice matched to the final layer of InAsP ($InAs_yP_{1-y}$ is lattice matched to $In_xGa_{1-x}As$ when $y=2.138x-1.138$). This process significantly reduces the effects of strain in the active region and produces high-quality InGaAs thin films. A passivation layer of InAsP was grown 30 nm thick on InGaAs. The thickness of the InGaAs layer in the double heterostructure was 0.37 μm for the 0.74 and 0.5 eV samples, and 0.15 or 0.30 μm for the 0.6 eV samples. The active InGaAs regions were n doped with sulfur.

We measured the lifetimes with a photoluminescence photon-counting technique. Because the photoluminescence from these samples was in the infrared, a sum-frequency up-conversion technique was required for photon counting.[9] The samples were pumped by 120 fs pulses at 82 MHz from a Spectra-Physics femtosecond mode-locked titanium-doped sapphire (Ti:S) laser running at 770 nm. The collected photoluminescence was mixed with the Ti:S laser pulse for sum-frequency generation (SFG) in a 1 mm lithium iodate ($LiIO_3$) crystal, and the SFG signal was dispersed by a SPEX 270 m spectrograph and detected by a Hamamatsu R464 photomultiplier tube. The system time resolution was about 130 fs. The free-carrier concentration was measured with the Van der Pauw–Hall technique.

Figure 1 illustrates the lifetime data. The lifetime varies roughly as the inverse square of the free-electron concentration, which is a primary indication that Auger recombination is dominant.

To determine the approximate ratio of radiative to non-

[a]Electronic mail: wyatt_metzger@nrel.gov

 © 2001 American Institute of Physics
Downloaded 02 Jun 2009 to 131.183.220.186. Redistribution subject to AIP license or copyright; see http://apl.aip.org/apl/copyright.jsp

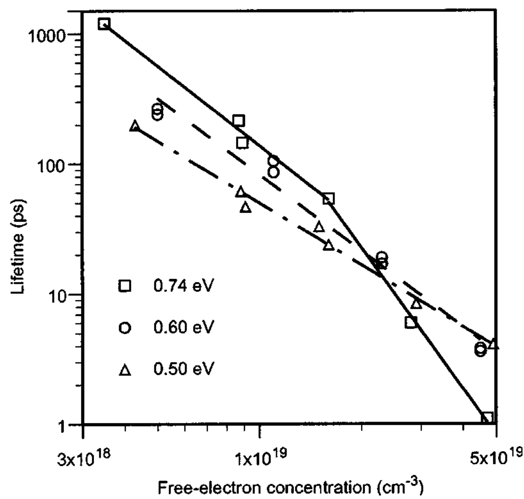

FIG. 1. Lifetime vs free-electron carrier concentration. The solid, dashed, and dashed-and-dotted lines represent the $\tau = An^x$ fits for the 0.74, 0.60, and 0.50 eV samples, respectively.

radiative recombination, we measured the photoluminescence (PL) intensity from each sample under steady-state low-injection conditions using a technique described in Ref. 10. The low-injection radiative external quantum efficiency (EQE) for n-type material is given by

$$\eta = \gamma R_r / R = \gamma B \tau n = \gamma I_{\mathrm{PL}} / I_0, \tag{2}$$

where γ is the ratio of external to internal radiative quantum efficiency; R_r and R are the radiative and the total rates of recombination, respectively; I_{PL} is the intensity of the photoluminescence; and I_0 is the intensity of the light absorbed by the semiconductor (not including thermalization).

We compared the PL intensity of these heavily doped samples with a 0.74 eV InGaAs sample n doped with 2.0×10^{17} electrons/cm^3. By assuming this sample is 100% efficient, we obtain a rough upper limit on the radiative quantum efficiency of the heavily doped samples. Figure 2 shows the PL intensity data. The low EQE indicates that radiative recombination is not a significant recombination mechanism.

Undoped samples made with the same growth technique and basic sample structure as these heavily doped samples have Shockley–Read–Hall lifetimes on the order of a

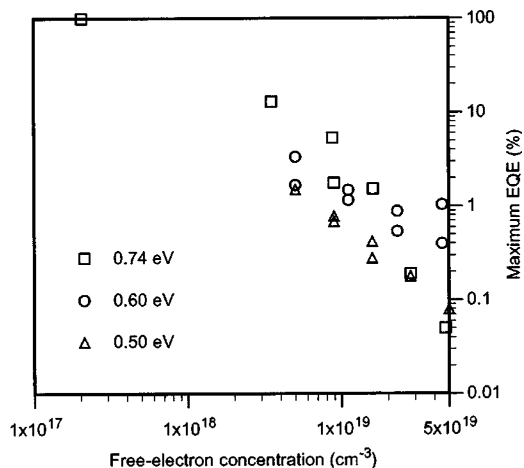

FIG. 2. Maximum EQE vs free-electron carrier concentration for three compositions.

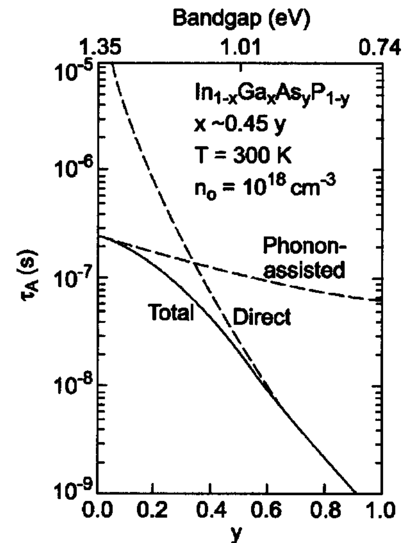

FIG. 3. Theoretical results of Dutta and Nelson (see Ref. 11) for InGaAsP lattice matched to InP. Phonon-assisted recombination changes far less with band gap than direct recombination.

microsecond.[3,11] Because the lifetimes of these heavily doped samples are inversely proportional to roughly the square of the free-electron density and are on the order of picoseconds, Shockley–Read–Hall recombination is considered insignificant.

The lifetime results were fit to the power law $\tau = An^x$. For the 0.60 and 0.50 eV samples, the best fits are given by $8.18 \times 10^{26}\ n^{-1.95}$ and $6.17 \times 10^{19}\ n^{-1.58}$, respectively. For the 0.74 eV data, the first four and the last three data points are best fit by $8.06 \times 10^{28}\ n^{-2.04}$ and $1.52 \times 10^{59}\ n^{-3.62}$, respectively.

There are very few theoretical treatments of Auger recombination that address the degree of degeneracy observed in these samples at 5×10^{19} carriers/cm^3. Spectral photoluminescence data on these samples and detailed ellipsometer studies on 0.6 eV InGaAs (Ref. 12) indicate that at 5×10^{19} carriers/cm^3, the Moss–Burstein shift becomes roughly as large as the intrinsic band gap and the Fermi level approaches the energy level of the L-band valley. However, Huag has studied how the lifetime should vary with carrier density in degenerate conditions for phonon-assisted, direct, and second-order Auger processes.[13] His results applied to low-injection conditions and n-type material give $\tau \sim n^{-1}$ for direct Auger recombination, $\tau \sim n^{-2}$ for phonon-assisted Auger recombination, and $\tau \sim n^{-7/3}$ for second-order processes. He claims that the direct Auger process is negligible for semiconductors with a band gap above 0.6 eV and that the effect of carrier degeneracy on phonon-assisted Auger recombination is weak until the carrier density exceeds 10^{20} carriers/cm^3.[14] Our results are consistent with Huag's conclusions.

A comparison of the values of exponent x in the data fits with the predictions of Huag indicates that the 0.60 eV ($x = -1.95$) and lightly doped 0.74 eV ($x = -2.04$) samples are dominated by phonon-assisted recombination. As the band gap is reduced to 0.50 eV, the smaller exponent, $x = -1.58$, suggests that direct Auger recombination may have a larger role, as is expected at smaller band gaps. At the highest carrier concentrations for the 0.74 eV material, a new

Downloaded 02 Jun 2009 to 131.183.220.186. Redistribution subject to AIP license or copyright; see http://apl.aip.org/apl/copyright.jsp

TABLE I. Theoretical values of the Auger coefficient for phonon-assisted and direct recombination.

Reference	16	17	18	19, 20
Material	0.74 eV InGaAs	0.74 eV InGaAs	0.95 eV InGaAsP	0.35 eV InAs
Direct (cm^6/s)	2×10^{-27}	3×10^{-29}	5×10^{-32}	6.6×10^{-27}
Phonon-assisted (cm^6/s)	2×10^{-29}	4×10^{-29}	6×10^{-29}	6.0×10^{-27}

effect, perhaps due to a higher-order process, impurity scattering, and/or band-structure effects, is required to explain the sudden increase in the Auger recombination rate. Similar behavior has been observed in heavily carbon doped p-GaAs, and was explained in part by the onset of impurity-assisted recombination.[10,15]

There are no rigorous theoretical calculations of Auger recombination for low-band-gap n-InGaAs with which to compare our results, but analysis of the theory available for weakly degenerate InGaAs and InAs provides more indications of phonon-assisted recombination. Figure 3 illustrates the predictions of Dutta and Nelson[16] for phonon-assisted and direct Auger recombination in the quaternary InGaAsP for weakly degenerate conditions ($n=10^{18}$ carriers/cm^3); the right-hand axis corresponds to 0.74 eV InGaAs. Their results clearly indicate that the Auger rate increases far more quickly as the band gap decreases for the direct process than it does for the phonon-assisted process.

Although theorists agree on this qualitative behavior, they disagree on the magnitude of the two processes, and on the band gap at which direct Auger recombination becomes larger than phonon-assisted Auger recombination for n-type InGaAs and InGaAsP [see Table I (Refs. 16–20) and Fig. 3]. The disagreement is typical in Auger theory and arises from the complexity of the problem, and in particular, the sensitivity of the calculation to the band model, wave functions, and approximations chosen by each author. Huag has pointed out that calculations of direct Auger recombination should be more sensitive to the specific band model than the calculations for phonon-assisted Auger recombination.

To compare our results to the literature, we used the expression, $\tau=1/Cn^2$, and found the Auger coefficient for passivated 0.74, 0.60, and 0.50 eV n-InGaAs to be 1.8, 1.2, and $0.7\times10^{-28}\,cm^6/s$, respectively. In the 0.74 eV data, the two data points at the highest doping concentration were omitted. The very small increase in the Auger rate with band gap is characteristic of phonon-assisted recombination, and the magnitude agrees fairly well with the theoretical estimates for phonon-assisted recombination. There is not enough theoretical work on impurity-assisted recombination for this material, nor for n-type strongly degenerate material in general, to determine what its role may be. But, the rate of Auger recombination, the slow decline of Auger recombination with band gap, and the dependence of the Auger rate on carrier density are all consistent with the theory for phonon-assisted recombination. It should be noted that heavy doping may make the role of phonon-assisted recombination more pronounced by increasing the number of phonon modes and limiting the number of direct transitions.[21] At lower band gaps and doping densities, direct Auger recombination tends to be more dominant. This could help explain why Auger recombination in InAs is so much larger than in 0.50 eV InGaAs.

In conclusion, the Auger recombination rate in low-band-gap InGaAs is far smaller than expected based on interpolation from InAs and $In_{0.53}Ga_{0.47}As$, and is consistent with the behavior predicted for the phonon-assisted process. This makes InGaAs a more attractive material for use in infrared detectors, thermophotovoltaic devices, laser diodes, and other minority-carrier devices.

[1] M. W. Wanlass, J. J. Carapella, A. Duda, K. Emery, L. Gedvilas, T. Moriarty, S. Ward, J. Webb, X. Wu, and C. S. Murray, AIP Conf. Proc. **460**, 132 (1998).
[2] C. H. Henry, R. A. Logan, F. R. Merritt, and C. G. Betha, Electron. Lett. **20**, 358 (1984).
[3] R. K. Ahrenkiel, R. Ellingson, S. Johnston, and M. Wanlass, Appl. Phys. Lett. **72**, 3470 (1998).
[4] K. L. Vodopyanov, H. Graener, C. C. Phillips, and T. J. Tate, Phys. Rev. B **46**, 13194 (1992).
[5] G. N. Galkin, F. F. Karakhorin, and E. V. Shatkovskii, Fiz. Tekh. Poluprovodn. (S.-Peterburg) **5**, 442 (1971).
[6] V. L. Dalal, W. A. Hicinbothem, Jr., and H. Kressel, Appl. Phys. Lett. **24**, 184 (1974).
[7] M. Osinski, P. G. Eliseev, V. A. Smagley, P. Uppal, and K. Ritter, *Proceedings of the 1997 Sensors and Electronic Devices Symposium, College Park, Maryland, 14–15 January 1997* (Environmental Research Institute of Michigan, Ann Arbor, MI, 1997), p. 7.
[8] G. P. Agrawal and N. K. Dutta, *Semiconductor Lasers* (Van Nostrand Reinhold, New York, 1993), Chap. 3.
[9] J. Shah, T. C. Damen, and B. Deveaud, Appl. Phys. Lett. **50**, 1307 (1987).
[10] R. K. Ahrenkiel, R. Ellingson, W. Metzger, D. I. Lubyshev, and W. K. Liu, Appl. Phys. Lett. **78**, 1879 (2001).
[11] R. K. Ahrenkiel, S. W. Johnston, J. D. Webb, L. M. Gedvilas, J. J. Carapella, and M. W. Wanlass, Appl. Phys. Lett. **78**, 1092 (2001).
[12] G. W. Charache, D. M. DePoy, J. E. Raynolds, P. F. Baldasaro, K. E. Miyano, T. Holden, F. H. Pollak, P. R. Sharps, M. L. Timmons, C. B. Geller, W. Mannstadt, R. Asahi, and A. J. Freeman, J. Appl. Phys. **86**, 452 (1999).
[13] A. Huag, Solid-State Electron. **21**, 1281 (1978).
[14] A. Huag, J. Phys. C **16**, 4159 (1983).
[15] M. Takeshima, Phys. Rev. B **23**, 771 (1981).
[16] N. K. Dutta and R. J. Nelson, J. Appl. Phys. **85**, 74 (1982).
[17] W. Bardyszewski and D. Yevick, J. Appl. Phys. **58**, 2713 (1985).
[18] A. Huag, Appl. Phys. Lett. **42**, 512 (1983).
[19] M. Takeshima, Jpn. J. Appl. Phys., Part 1 **22**, 491 (1983).
[20] M. Takeshima, J. Appl. Phys. **46**, 3082 (1975).
[21] P. T. Landsberg, Solid-State Electron. **30**, 1107 (1987).

Downloaded 02 Jun 2009 to 131.183.220.186. Redistribution subject to AIP license or copyright; see http://apl.aip.org/apl/copyright.jsp